

ESR study of the concentrated spin glass *a*-MnSi

M. C. Aronson and M. B. Salamon

*Department of Physics and Materials Research Laboratory,
University of Illinois at Urbana-Champaign, Urbana, Illinois 61801*

J. J. Hauser

AT&T Bell Laboratories, Murray Hill, New Jersey 07974

(Received 17 March 1986)

We have measured the ESR linewidth, W , and shift, ΔH , in amorphous MnSi at 9.35 GHz and temperatures below 70 K. Above the spin-glass transition temperature $T_g=24$ K, we find $W \propto \Delta H^{0.5}$. Although this relationship usually is the signature of the extreme dynamic narrowing limit, the experimental values of W and ΔH indicate that static fields are of major importance over the complete temperature range in *a*-MnSi. Using the Kubo-Toyabe model, we find a temperature-independent random field strength of 2.6×10^{10} s⁻¹ and a temperature-dependent spin relaxation time τ which scales as $\tau \propto T_g/(T - T_g)$. These results show that spin relaxation in *a*-MnSi is dominated by the strength of the random fields, not by dynamic narrowing.

I. INTRODUCTION

Amorphous MnSi is a concentrated spin glass, in which competing spin interactions arise from structural disorder.¹ However, both magnetization²⁻⁴ and neutron scattering measurements⁵ indicate that its spin-glass transition has the same qualitative features of the more familiar dilute metallic spin glasses. In view of these results, it is interesting to investigate the relationship between spin relaxation and the development of spin-glass order in *a*-MnSi, with emphasis on features related to the concentrated nature of *a*-MnSi. Consequently, we report here the results of an electron spin resonance (ESR) experiment on *a*-MnSi at temperatures both above and below the spin-glass transition. Our results not only describe the relationship between high- and low-temperature linewidth and resonance field, but also detail the relative importance of random anisotropy fields and exchange narrowing in determining the spin relaxation in *a*-MnSi.

II. EXPERIMENTAL DETAILS

Samples of amorphous MnSi were prepared by a getter sputtering technique describe in detail by Hauser and co-workers.^{2,3} The temperature of the substrate greatly affects the formation of microcrystalline clusters in the films. X-ray diffraction and scanning electron microscopy were used to confirm that the samples used in the ESR experiment were highly amorphous. In addition, an extended x-ray absorption fine-structure (EXAFS) experiment¹ performed on a similar sample found no evidence for Mn-Mn clustering, and showed a broad distribution of Mn-Si spacings centered about 2.43 Å. The spin-glass transition temperature, T_g , was determined to be 24 K from the peak in the ac susceptibility, which was measured at 10 kHz.^{2,3}

The ESR experiments reported here were performed on approximately 2 g of *a*-MnSi flakes, from the same batch

that provided the neutron scattering sample.⁵ The flakes were mixed with quartz powder to disperse the sample evenly in the cavity, and to optimize the microwave power absorption. ESR was performed at 9.35 GHz on a Bruker ER200D spectrometer with 100-kHz field modulation. The sample temperature was monitored with a calibrated Au-Fe thermocouple located about 1.5 cm from the sample tube in the cold helium-gas flow.

Above 30 K, the derivative line shapes were moderately well fitted by an admixture of real and imaginary parts of the dynamic susceptibility, which was assumed to be Lorentzian. The degree of admixture of the real and imaginary parts of the susceptibility was determined from the experimental A/B ratio;⁶ the mixing parameter was 0.44, independent of temperature. Since the lines are relatively broad, the negative frequency spectral contribution was included in the computer fit. The resonant field, H_0 , and linewidth, $W = 1/\gamma_0 T_2$, where $\gamma_0 = g\mu_B/\hbar$, were used as fitting parameters; their temperature dependence is shown in Figs. 1 and 2. Although a resonance was ob-

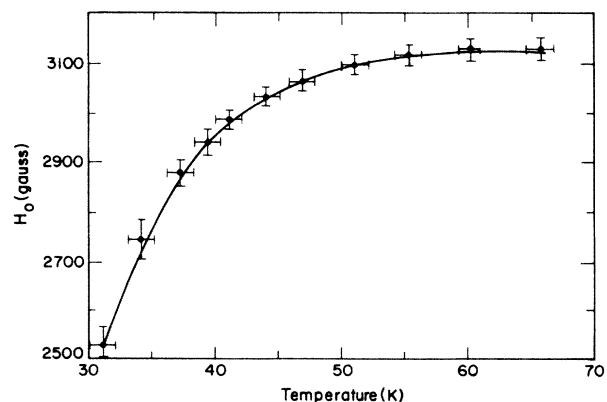


FIG. 1. Temperature dependence of the resonance field. Solid line is a guide to the eye.

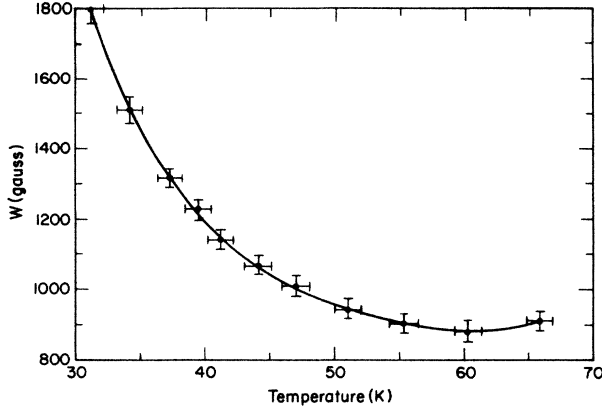


FIG. 2. Temperature dependence of the linewidth. Solid line is a guide to the eye.

served down to 3.7 K, extreme broadening and distortion of the experimental line shape rendered the fit inaccurate below 30 K.

The resonant field and linewidth show the behavior generally observed in ESR experiments on dilute spin glasses;⁷⁻¹³ they are roughly temperature independent at high temperature, but change rapidly for $T \leq 2T_g$. Assuming a linear relationship between the resonant field and frequency, we extract the effective fractional g shift shown in Fig. 3. The high-temperature linewidth and g shift in a spin glass are usually the result of Korringa processes, but at lower temperatures the ESR parameters may be related to dynamic processes and static fields. We shall treat each of these cases in turn.

III. HIGH-TEMPERATURE ESR RESULTS: THE KORRINGA CONTRIBUTION

Above 55 K, the resonance is characterized by an average g factor of 2.15, and an average linewidth W of 880 G. The data show only a weak temperature dependence for Δg and W over this temperature range: $dW/dT \leq 7$ G/K, and $d\Delta g/dT \leq 0.005$. We use these parameters to

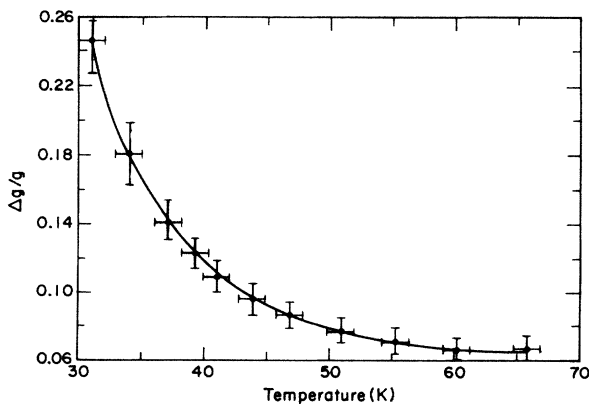


FIG. 3. Temperature dependence of the fractional g shift, assuming $\hbar\omega^{\text{res}} = g\mu_B H^{\text{res}}$. The shift is measured from $g = 1.998$. Solid line is a guide to the eye.

obtain a more detailed picture of the high-temperature metal.

EXAFS experiments have shown that the Mn ions in amorphous MnSi have only Si ions as nearest neighbors.¹ Consequently, the Mn-Mn exchange interactions are indirect, and mediated by the conduction electrons. The interaction energy, E_{ij} , may be described by the Ruderman-Kittel-Kasuya-Yosida (RKKY) theory.¹⁴

$$E_{ij} = -2J_{ij}S_i \cdot S_j, \quad (1)$$

$$J_{ij} = \frac{9}{8} \frac{n_0^2 \pi}{E_F} J_{sd}^2 F(2k_F r_{ij}), \quad (2)$$

$$F(q) = \frac{1}{q^4} [\sin(q) - q \cos(q)], \quad (3)$$

where n_0 is the number of conduction electrons per atom, k_F is the Fermi wave vector, E_F is the Fermi energy, S_i is the Mn spin, J_{sd} is the zero momentum component of the interaction integral between the localized spin and the conduction electron spin, and r_{ij} is the spacing of Mn spins.

We use a nearly-free-electron estimate of the Fermi energy, E_f , and coupling integral, J_{sd} , to calculate the RKKY strength, J_{ij} . Assuming that the Mn ions are in the Mn^{2+} configuration, with an average Mn-Mn spacing¹ of 2.7 Å and a Curie temperature³ of 30 K, we obtain a nearest-neighbor RKKY strength $J_{ij} = 0.15$ meV. Since J_{ij} is positive, a majority of the Mn-Mn interactions are ferromagnetic, consistent with the observation of a positive Curie temperature. However for the average Mn nearest-neighbor spacing, J_{ij} is very close to the first RKKY zero crossing; only small fluctuations in Mn concentration are required to form regions where J_{ij} is negative. It is likely that this competition between ferromagnetic and antiferromagnetic coupling is the source of spin-glass behavior in α -MnSi.

Using the RKKY formalism, we can calculate the high-temperature Korringa relations, assuming there is no bottle neck.

$$\Delta g = \frac{3n_0 J_{sd}}{4E_f} \gtrsim 0.06, \quad (4)$$

$$\frac{dW}{dT} = \frac{\pi \Delta g^2 k_B}{g\mu_B} \gtrsim 8 \text{ G/K}. \quad (5)$$

Although dW/dT is consistent with the present experiment, the g shift is almost a factor of 3 smaller than observed. This discrepancy might be resolved by including some d -like character in the conduction band and consequently increasing the density of states at the Fermi surface. Alternatively, since the angular momentum state of the Mn ions is not known, it is possible they are not in the Mn^{2+} Hund's-rule ground state. However, we will show in the next section that the high-temperature linewidth and shift, while including a small Korringa contribution, are predominantly the result of a temperature-independent anisotropy field, narrowed by a temperature-dependent exchange process.

IV. LOW-TEMPERATURE ESR RESULTS: THE KUBO-TOYABE MODEL

ESR lines in spin glasses characteristically broaden and shift to lower resonance fields as the temperature decreases towards T_g . In general, this temperature dependence is the result of both static and dynamic processes. The resonant moments in a spin glass are perturbed by a time-dependent anisotropic interaction $\mathbf{H}(t)$ of either dipolar⁷ or Dzyaloshinskii-Moriya¹⁵ origin. In both cases, the exchange interaction modulates $\mathbf{H}(t)$ at a rate $1/\tau$, reducing the effectiveness of $\mathbf{H}(t)$ in broadening the resonance. The exchange rate $1/\tau$ can be best understood in terms of a strong collision model.¹⁶ Here, the spin system is subject to a static perturbation for a time τ , after which the perturbation jumps to a new random orientation. The extent to which this modulation $\mathbf{H}(t)$ results in exchange narrowing depends on the relative sizes of the resonance frequency ω_0 , the magnitude of $\mathbf{H}(t)$, and the exchange rate $1/\tau$.

Formally, the Kubo-Toyabe model^{16,17} describes the time evolution of a spin system in which spins precess in the resultant of the applied field and a time varying random field $\mathbf{H}(t)$. The instantaneous values of $|\mathbf{H}(t)|$ are described by a Gaussian of width Δ/γ_0 , centered at zero field. The field autocorrelation function is assumed to be given by:

$$\langle \mathbf{H}(t+\tau) \cdot \mathbf{H}(\tau) \rangle = 3 \left[\frac{\Delta}{\gamma_0} \right]^2 \exp \left[-\frac{t}{\tau} \right]. \quad (6)$$

We note that this model is only approximately valid in a spin glass, where power law decays are predicted.¹⁸ Despite this qualification, we describe the temperature dependence of the *a*-MnSi linewidth and shift in terms of Δ and τ of the Kubo-Toyabe model.

Unlike conventional approaches, the Kubo-Toyabe model is valid from the fast modulation ($\Delta\tau \ll 1$) region, where the resonance occurs near the intrinsic g factor and is strongly narrowed by dynamic effects, to the slow modulation region ($\Delta\tau \gg 1$) where both the resonance field and linewidth are dominated by Δ/γ_0 . In the intermediate region neither static random fields nor exchange narrowing adequately describe the resonance response. Physical interpretation of the resonance in this region is complicated by the mixing of the secular and nonsecular contributions, and when the random fields are comparable to the applied field, by the need to treat the Zeeman splitting and the quasistatic field splitting on equal grounds. In light of these complications, we have used computed Kubo-Toyabe line shapes^{16,19} to extract the Δ and τ dependence of the half-widths, W , and resonance field shifts, $2\pi f/\gamma_0 - H_0$, where f is the experimental microwave frequency. We introduce the dimensionless parameters $W' = (\gamma_0 W)/(2\pi f)$, $H' = (\gamma_0 H_0)/(2\pi f)$, $\Delta' = \Delta/2\pi f$, and $\tau' = 2\pi f\tau$. Figure 4 shows the relationships for W' and $(1-H'_0)$ along lines of constant Δ' and constant τ' ; Fig. 5 is an expanded view of lines of constant Δ' for linewidths and shifts near the static limit ($\tau' \rightarrow \infty$). The scaled *a*-MnSi data are plotted on each figure for comparison. In the fast modulation region, we regain the result of the Mori-Kawasaki theory:²⁰ $W' \propto 1/T_2 \propto \Delta'^2 \tau'$

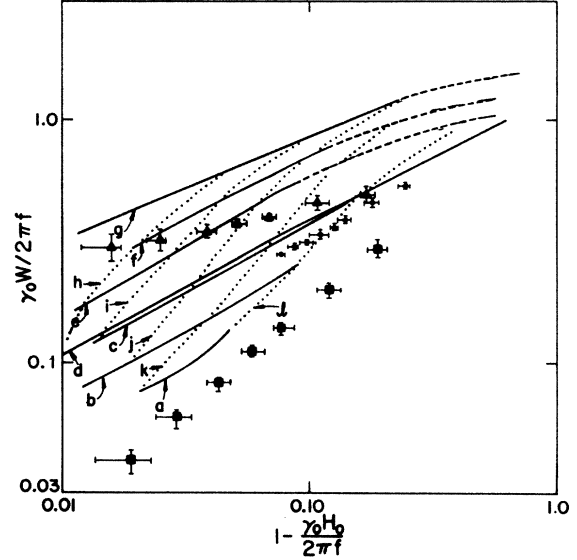


FIG. 4. Δ' and τ' dependence of the resonance linewidth and shift in the Kubo-Toyabe model. Solid lines are lines of constant $\Delta' = \Delta/(2\pi f)$. *a*, $\Delta' = 0.25$; *b*, $\Delta' = 0.35$; *c*, $\Delta' = 0.5$; *e*, $\Delta' = 0.75$; *f*, $\Delta' = 1.0$; *g*, $\Delta' = 1.5$. Dotted lines are lines of constant $\tau' = 2\pi f\tau$. *d*, $\tau' = \infty$; *h*, $\tau' = 0.15$; *i*, $\tau' = 0.25$; *j*, $\tau' = 0.45$; *k*, $\tau' = 0.75$; *l*, $\tau' = 2.15$. The dashed lines indicate extrapolation from the numerical results. The meaning of the different data points is discussed in the text. All field strengths and relaxation times are scaled by the experimental microwave frequency, f .

and $(1-H'_0) \propto \Delta g/g \propto \Delta'^2 \tau'^2$, giving $W' \propto (1-H'_0)^{1/2}$. In the static limit, however, $W' \propto \Delta'$ and $(1-H'_0) \propto \Delta'^2$, so that again $W' \propto (1-H'_0)^{1/2}$.

Since the Kubo-Toyabe model only describes the contributions of dipolar or Dzyaloshinskii-Moriya processes, we have subtracted the free-electron estimate of the Korringa shift from the experimental data, and plotted the results as solid circles in Fig. 4. The data are well described by the Kubo-Toyabe model using the parameters $\Delta' = 0.45 \pm 0.03$ and $0.9 \leq \tau' \leq 2.5$.

An alternative analysis, shown as solid squares in Fig. 4, assumes that the high-temperature g shift is all due to

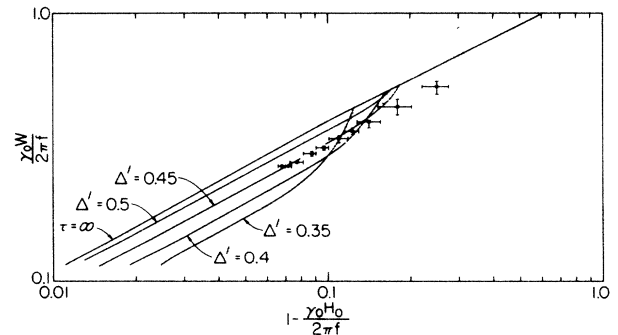


FIG. 5. Δ' and τ' dependence of the resonance linewidth and shift near the static limit of the Kubo-Toyabe model. The solid circles are the *a*-MnSi data with a 98-G Korringa shift subtracted. The dashed lines indicate extrapolation from the numerical results. All field strengths and relaxation times are scaled by the experimental microwave frequency, f .

the conduction electrons and uses the Korringa relation to subtract the corresponding contribution to the width. We can immediately dismiss a Korringa shift of this magnitude, since it causes the *a*-MnSi data to fall outside the range possible in the Kubo-Toyabe model. Another possibility, more difficult to reject, is that the high-temperature excess shift is the result of a static anisotropy field, such as those previously invoked to explain resonance modes in spin glasses at temperatures well below the spin-glass transition.²¹ An anisotropy field H_i of 680 ± 50 G would shift the resonance field H_R from the true resonance field, $2\pi f/\gamma_0$, to the observed high-temperature value, according to:²²

$$2\pi f/\gamma_0 = \frac{1}{2}H_R + \frac{1}{2}(H_R^2 + 4H_i^2)^{1/2}. \quad (7)$$

The shifted *a*-MnSi data are plotted as solid triangles in Fig. 4. Although the data fall in an allowed range of the model, they are not readily described by lines of constant Δ' , τ' , or $\Delta'\tau'$. Nonetheless, we cannot rule out a static anisotropy field solely from the Kubo-Toyabe model. However, it is unlikely that the remanence-induced anisotropy field observed in spin glasses persists so far above the spin-glass transition.

We conclude that the random field strength Δ' in *a*-MnSi is almost temperature independent, while the spin-relaxation time τ increases as the temperature is decreased. As the temperature approaches T_g from above, the random field strength departs somewhat from the constant value $\Delta' = 0.45$, significantly increasing our uncertainty in τ' for temperatures less than ~ 34 K. This departure might be explained either as a breakdown of the exponential time decays of the random field autocorrelation function near T_g , by the emergence of a remanence-induced static anisotropy field near T_g , or by the χ^{-1} dependence of Δ/γ_0 .¹⁹

The temperature dependence of τ' has an interesting consequence in view of the neutron scattering results.⁵ In that experiment, the temperature dependence of the spin-relaxation rate $\Gamma(T)$ was proposed to have either an Arrhenius form

$$\Gamma(T) = \Gamma_0 \exp\left[\frac{-T_0}{T}\right] \quad (8)$$

or a critical scaling form

$$\Gamma(T) = \Gamma_0' \left[\frac{T - T_g}{T_g}\right]. \quad (9)$$

The temperature dependence of the inelastic neutron scattering width was best fit using $\Gamma_0 = 1.4 \times 10^{12} \text{ s}^{-1}$, $\Gamma_0' = 2.1 \times 10^{11} \text{ s}^{-1}$, and $T_0 = 73$ K.

The temperature dependences of $2\pi f/\Gamma(T)$ and $\tau'(T)$ are shown in Fig. 6. Below ~ 55 K, the ESR relaxation times for *a*-MnSi are equally well fit by either an Arrhenius form

$$\tau(T) = \tau_0 \exp\left[\frac{T_0'}{T}\right] \quad (10)$$

or a critical scaling form

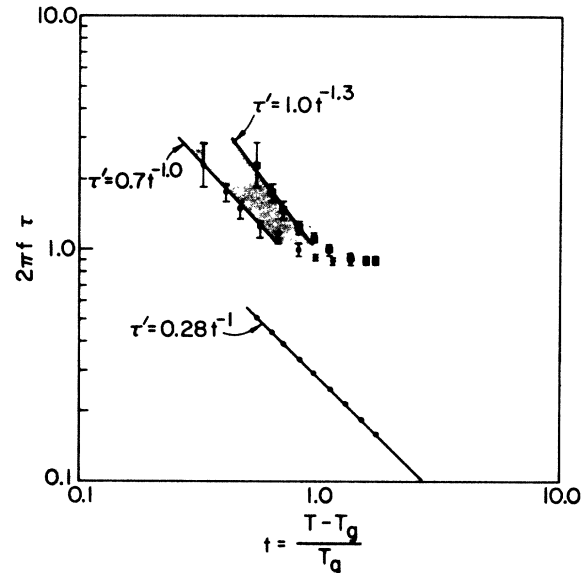


FIG. 6. Reduced temperature dependence of the ESR spin-relaxation time τ' . The shaded region gives values of τ' permitted by uncertainty in the reduced temperature. The line $\tau' = 1.0t^{-1.3}$ assumes $T_g = 24$ K, while the line $\tau' = 0.7t^{-1.0}$ takes $T_g = 28$ K. The line $(2\pi f)/\Gamma(t) = 0.28t^{-1}$ gives the reduced temperature dependence of the neutron scattering spin-relaxation time (Ref. 5).

$$\tau(T) = \tau_0' \left[\frac{T_g}{T - T_g}\right]^x. \quad (11)$$

Taking into account experimental uncertainties in temperature and τ , our data are fit by parameters falling within the following ranges: $x = 1.15 \pm 0.15$, $\tau_0' = (1.45 \pm 0.25) \times 10^{-11} \text{ s}$, $\tau_0 = (3.85 \pm 0.45) \times 10^{-12} \text{ s}$, and $T_0' = 76.5 \pm 6.5$ K. Since neutron scattering experiments measure a two-spin correlation function and ESR experiments measure a four-spin correlation function, we cannot simply relate $1/\Gamma(T)$ and $\tau(T)$ of the Kubo-Toyabe model. However, we find that $2\pi f/\Gamma(T)$ and $\tau'(T)$ are of the same order of magnitude, over the temperature range of the ESR experiment. Although the relationship between two-spin and four-spin correlation functions is the subject of continuing theoretical controversy,^{7,15} numerical differences between their decay rates are to be expected. Since $\tau(T)$ and $1/\Gamma(T)$ are comparable, it is reasonable that the neutron scattering and ESR experiments are probing qualitatively similar relaxation modes. Naively, one expects a four-spin relaxation time to be shorter than a two-spin relaxation time, in contrast to what we observe in *a*-MnSi. This discrepancy is most simply resolved by noting that the ESR experiment is performed with $q \approx 0$, while the neutron scattering experiment has $q = 0.16 \text{ \AA}^{-1}$. Murani^{23,24} has found that the quasielastic neutron scattering width $\Gamma(q)$ increases with increasing momentum transfer for several dilute spin glasses, both above and below the freezing temperature. If this trend can be extrapolated to concentrated spin glasses, then it is reasonable for the $q \approx 0$ ESR relaxation time to be longer than Γ^{-1} ($q = 0.16 \text{ \AA}^{-1}$). However, this extra-

TABLE I. Spin-glass transition temperatures, ESR relaxation times, and static field strengths for some dilute and concentrated spin glasses. Entries with an asterisk are in the extreme narrowing limit. In each material, $\tau(T) = \tau_0 [T_g / (T - T_g)]$.

Spin glass	T_g (K)	τ_0 (s)	Δ (s ⁻¹)	$\Delta\tau_0$	Reference
Cu ₉₆ Mn ₄ *	23	7.1×10^{-12}	0.8×10^{10}	0.06	12
Cu ₇₅ Mn ₂₅ *	120	1.1×10^{-12}	4×10^{10}	0.04	7
Mg ₉₉₅ Mn ₅ *	2.9	5.0×10^{-11}	1×10^{10}	0.5	13
Gd ₃₇ Al ₆₃ *	14	5.0×10^{-12}	7×10^{10}	0.35	14
Fe ₁₀ Ni ₇₀ P ₂₀	23	4.3×10^{-11}	3×10^{10}	1.3	19
a -MnSi	24	1.2×10^{-11}	2.6×10^{10}	0.3	This work
Fe ₁₆ Ni ₆₄ P ₂₀	15	1.4×10^{-11}	3.5×10^{10}	0.5	25

polarization is of questionable validity, since Murani^{23,24} finds the apparent freezing temperature to increase with decreasing q , while Aeppli *et al.*⁵ find a higher T_g than the $q \approx 0$ measurements.^{2,3} Measurement of the q dependence of $\Gamma(q)$ for a -MnSi is required to resolve this issue.

Although the scaling form

$$\tau = \tau'_0 \left(\frac{T_g}{T - T_g} \right) \quad (12)$$

is not characteristic of all spin glasses, it has been observed in a wide range of dilute and concentrated metallic spin glasses. The ESR relaxation times and anisotropy field strengths for some representative materials are listed in Table I. The most striking feature is that τ_0 and Δ vary by less than an order of magnitude, regardless of spin-glass type. It has been claimed that the materials in Table I marked with an asterisk are in the extreme narrowing limit, while full Kubo-Toyabe analysis has been applied to the remaining entries. If the extreme narrowing claims are correct, then the spin-relaxation dynamics must be very sensitive to Δ and τ_0 . Further, the critical behavior of τ near T_g must certainly cause the narrowing limit to break down in these materials. As we observed, a quadratic relationship between resonance linewidth and shift is the signature of both the extreme narrowing ($\Delta\tau \ll 1$) and static ($\tau \rightarrow \infty$) limits; careful line-shape analysis must be used to correctly determine the dynamic regime.

A more detailed inspection of Table I shows that a -MnSi has a Δ and τ_0 closer to those of the concentrated materials a -GdAl₂, Fe₁₆Ni₆₄P₂₀, and Fe₁₀Ni₇₀P₂₀ than to the dilute spin glass Cu₉₆Mn₄. Although the dilute spin glasses tend to have shorter τ_0 and smaller Δ than the concentrated spin glasses, this generalization cannot be pushed too far. We note that dilute Mg₉₉₅Mn₅ has Δ and τ_0 close to those of a -MnSi, while concentrated Cu₇₅Mn₂₅ has $\Delta\tau_0$ close to that of Cu₉₆Mn₄. Apparently, a complete

explanation of the relationship between spin relaxation and spin concentration in spin glasses must also include consideration of microscopic details.

V. CONCLUSIONS

Qualitatively, a -MnSi has the same ESR behavior as other dilute and concentrated spin glasses; the resonance broadens and shifts to lower fields, and the spin-relaxation time diverges as the temperature is decreased towards T_g . Over the complete temperature range studied, the spin relaxation in a -MnSi is dominated by the strength of the random anisotropic fields, not by dynamic narrowing. Since the dynamic narrowing condition is not satisfied in a -MnSi, we cannot use the Mori-Kawasaki formalism to describe the resonance. Instead, we use the Kubo-Toyabe model to interpret the temperature dependence of the ESR parameters.

Both neutron scattering and ESR experiments observe a power-law dependence of the spin-relaxation time for $T \geq T_g$. Since the two-spin correlation time measured by neutron scattering is always shorter than the four-spin correlation time measured by the ESR experiment, we suggest that the spin-correlation times in this concentrated spin glass are q dependent.

In conclusion, we have presented evidence that a -MnSi behaves like a true spin glass, and that its spin relaxation is more similar to that of concentrated spin glasses than dilute spin glasses.

ACKNOWLEDGMENTS

We are grateful to Dr. T. A. L. Ziman for generating the line-shape programs. The work at the University of Illinois was supported by the Materials Research Laboratory through Grant No. DMR-8316981.

¹J. M. Hayes, J. W. Allen, J. B. Boyce, and J. J. Hauser, Phys. Rev. B **23**, 4691 (1981).

²J. J. Hauser, Solid State Commun. **30**, 201 (1979).

³J. J. Hauser, F. S. L. Hsu, G. W. Kammlott, and J. V. Waszczak, Phys. Rev. B **20**, 3391 (1979).

⁴J. J. Hauser and R. J. Felder, Phys. Rev. B **27**, 4376 (1976).

⁵G. Aeppli, J. J. Hauser, G. Shirane, and Y. J. Uemura, Phys. Rev. Lett. **54**, 843 (1985).

⁶M. Peter, D. Shaltiel, J. H. Wernick, H. J. Williams, J. B. Mock, and R. C. Sherwood, Phys. Rev. **126**, 1395 (1962).

⁷M. B. Salamon and R. M. Herman, Phys. Rev. Lett. **41**, 1506 (1978); M. B. Salamon, Solid State Commun. **31**, 781 (1979).

- ⁸G. Mozurkewich, J. Elliot, M. Hardiman, and R. Orbach, *Phys. Rev. B* **29**, 278 (1984).
- ⁹K. Babersche, C. Pappa, H. Mahdjour, and R. Wendler, *J. Magn. Magn. Mater.* **54-57**, 179 (1986).
- ¹⁰Wei-Yu Wu, G. Mozurkewich, and R. Orbach, *Phys. Rev. B* **31**, 4557 (1985).
- ¹¹R. W. Tustison, *Solid State Commun.* **19**, 1075 (1976).
- ¹²D. Griffiths, *Proc. Phys. Soc., London*, **90**, 707 (1967).
- ¹³F. W. Kleinhans and P. E. Wigen, *Magnetism and Magnetic Materials—1971 (Chicago)*, Proceedings of the 17th Annual Conference on Magnetism and Magnetic Materials, AIP Conf. Proc. **5**, edited by D. C. Graham and J. J. Rhyne (AIP, New York, 1971), p. 1204. It has not been conclusively shown that the onset of antiferromagnetic resonance at 9 K in this alloy is due to spin-glass ordering.
- ¹⁴J. P. Jamet and A. P. Malozemoff, *Phys. Rev. B* **18**, 75 (1975).
- ¹⁵P. M. Levy, C. Morgan-Pond, and R. Raghavan, *Phys. Rev. Lett.* **50**, 1160 (1983).
- ¹⁶R. Kubo and T. Toyabe, in *Magnetic Resonance and Relaxation*, edited by R. Blinc (North-Holland, Amsterdam, 1967), p. 810.
- ¹⁷R. S. Hayano, Y. J. Uemura, I. Imazoto, N. Nishida, T. Yamazaki, and R. Kubo, *Phys. Rev. B* **20**, 850 (1979).
- ¹⁸H. Sompolinsky and A. Zippelius, *Phys. Rev. Lett.* **47**, 359 (1981).
- ¹⁹M.-K. Hou, M. B. Salamon, and T. A. L. Ziman, *Phys. Rev. B* **30**, 5239 (1984). There are several errors in the expression for the static linewidth in this paper. The correct expression should be taken directly from Ref. 16 of the present work.
- ²⁰H. Mori and K. Kawasaki, *Prog. Theor. Phys.* **27**, 529 (1962).
- ²¹S. Schultz, E. M. Gullikson, D. R. Fredkin, and M. Tovar, *J. Appl. Phys.* **52**, 1776 (1981).
- ²²C. L. Henley, H. Sompolinsky, and B. I. Halperin, *Phys. Rev. B* **25**, 5849 (1982).
- ²³A. P. Murani, *Phys. Rev. Lett.* **41**, 1406 (1978).
- ²⁴A. P. Murani, *J. Appl. Phys.* **49**, 1604 (1978).
- ²⁵M.-K. Hou, M. B. Salamon, and M. J. Pechan, *J. Appl. Phys.* **57**, 3482 (1985).

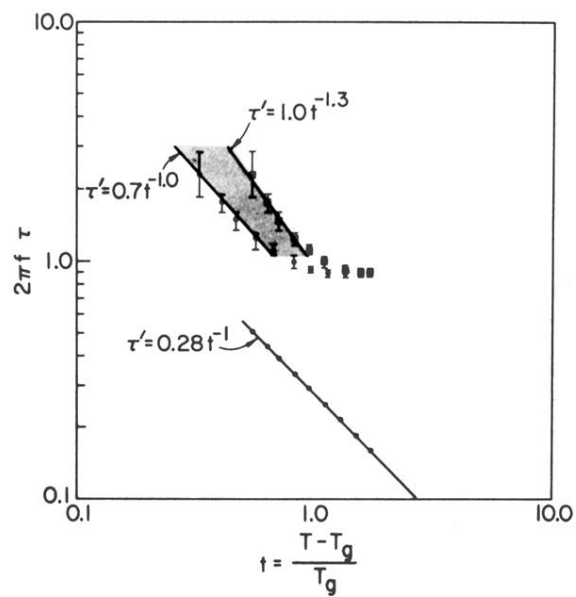


FIG. 6. Reduced temperature dependence of the ESR spin-relaxation time τ' . The shaded region gives values of τ' permitted by uncertainty in the reduced temperature. The line $\tau' = 1.0t^{-1.3}$ assumes $T_g = 24$ K, while the line $\tau' = 0.7t^{-1.0}$ takes $T_g = 28$ K. The line $(2\pi f)/\Gamma(t) = 0.28t^{-1}$ gives the reduced temperature dependence of the neutron scattering spin-relaxation time (Ref. 5).